Newtonian and Relativistic Plasmas: Acceleration mechanisms in GRBs

INTRODUCTION TO PLASMA DYNAMICS

Author:
Luca Pezzini
Jeroen Van den Bosch
Tinatin Baratashvili
Nimmy Samson Attipetty
Ozkann Gurhn

Supervisor:
Fabio Bacchini

MSc Astrophysics

KU Leuven, Physics department
October 14, 2020

1 Introduction

Stability is an important concept in Plasma Physics. The deviation from the stable state or equilibrium state results in accumulation of energy. The generation of instability is a way of redistributing this accumulated energy in the non equilibrium state [1]. The deviations from non equilibrium state occurs when certain parts of the plasma in equilibrium is acted upon by perturbative forces. These perturbations will then grow or damp out or oscillate. In this report we present our study of two instabilities namely, the two stream and the filamentation instability.
We start our study of instabilities first with the one dimensional Newtonian electrostatic two stream instability. We then apply the same to the relativistic case followed by a generalized approach in deriving the instabilities for counter streaming plasmas. Aforementioned instabilities are common in many astrophysical plasmas and are often invoked to explain events like gamma ray bursts and shock formation in the supernova remnants. Relativistic two stream instability was proposed as a possible mechanism to generate strong magnetic fields in the collisionless shocks of gamma ray bursts (GRB)[2].These bursts are thought to be cosmological and are believed to be produced in extremely energetic events. Within a fraction of few seconds an enormous amount energy is released from a small volume. The radiation observed in the GRB's are produced by accelerated electrons which cool through the inverse Compton process.Whereas the after glow radiation is produced through synchrotron radiation in the after shock magnetic fields which can be external(interaction with interstellar medium) or internal(through collisions).To explain the observational data, the strong magnetic fields have to be present in plasma at all times which is thought to be produced by the instabilities under consideration. Wave particle interaction can lead to a growing wave amplitude which results in two stream instability [3]. In this study we consider only a simple case of two stream instability.Two stream instability is said to be electrostatic as the wave number and electric field are aligned.Hence it can be seen from Faraday's law that $\mathbf{k}\times\mathbf{E}=\frac{\omega}{c}\mathbf{E}$ that this type of instability does not generate magnetic fields. Filamentation instability is electromagnetic in nature.In this case, the magnetic field generation is maximum for a given value of **kE** as **E** and **k** are perpendicular. According to Fried this instability can be understood in terms of superposition of many counter streaming beams [4].

2 Newtonian, electrostatic two-stream instability

In this case we are considering a simple case of one dimensional system where two electron beams of equal density are counter streaming say in the x-direction. Initially the state is in equilibrium. The quantities characterizing this state are, the number of particles, $n_r = n_l = n_0$, the particle velocities $\mathbf{v}_r = -\mathbf{v}_l = \mathbf{v}_0$ and electric field $E_0 = 0$.In this case magnetic field is assumed to be zero. There are also an additional background of immobile ions which remain immobile throughout the evolution of the system. Consider the Euler and Poisson's equations for each population s.

$$\frac{\partial n_s}{\partial t}+\frac{\partial(n_s,v_s)}{\partial x}=0 \tag{1}$$

$$m_s\frac{\partial(v_s)}{\partial t}+m_s v_s\frac{\partial v_s}{\partial x}=q_sE \tag{2}$$

$$\frac{\partial E}{\partial x}=\sum_s\frac{q_s n_s}{\varepsilon_0} \tag{3}$$

n_s, v_s are the number density and velocity and m_s and q_s are the particle mass and charge. For simplicity we assume units in which $\varepsilon_0 = 1$. The system is now perturbed. The perturbed quantities are now,

$$n_s \to n_{s,0}+n_{s,1}(x,t) \tag{4}$$

$$v_s \to v_{s,0}+v_{s,1}(x,t) \tag{5}$$

$$E \to E_0+E_1(x,t) \tag{6}$$

Introducing these quantities in the Euler and Poisson's equations and ignoring higher order perturbed terms results in the linearized evolution equations.For the right streaming beam,

$$\frac{\partial n_{r,1}}{\partial t}+n_0\frac{\partial v_{r,1}}{\partial x}+v_0\frac{\partial n_{r,1}}{\partial x}=0 \tag{7}$$

$$ms\frac{\partial v_{r,1}}{\partial t}+m_s v_0\frac{\partial v_{r,1}}{\partial x}=q_sE_1 \tag{8}$$

For left streaming beam,

$$\frac{\partial n_{l,1}}{\partial t} + n_0 \frac{\partial v_{l,1}}{\partial x} + v_0 \frac{\partial n_{l,1}}{\partial x} = 0 \tag{9}$$

$$ms\frac{\partial v_{l,1}}{\partial t} - m_s v_0 \frac{\partial v_{l,1}}{\partial x} = q_s E_1 \tag{10}$$

$$\frac{\partial E_1}{\partial x} = \sum q_s (n_{l,1} + n_{r,1}) \tag{11}$$

Considering a wave like behaviour for all the perturbed terms,

$$n_1(x,t) \propto \tilde{n_1} \exp^{i(kx-\omega t)} \tag{12}$$

$$v_1(x,t) \propto \tilde{v_1} \exp^{i(kx-\omega t)} \tag{13}$$

$$E_1(x,t) \propto \tilde{E_1} \exp^{i(kx-\omega t)} \tag{14}$$

An Euler and Laplace transform of the above equations results in the following set of equations.

$$n_0 k\widetilde{v_{r_1}} = \widetilde{n_{r,1}}(\omega - v_0 k) \tag{15}$$

$$-im_s\omega\widetilde{v_{r,1}} + m_s v_0 ik\widetilde{v_{r,1}} = q_s E_1 \tag{16}$$

$$n_0 k\widetilde{v_{l_1}} = \widetilde{n_{l,1}}(\omega + v_0 k) \tag{17}$$

$$im_s\omega\widetilde{v_{l,1}} + m_s v_0 ik\widetilde{v_{l,1}} = q_s\widetilde{E_1} \tag{18}$$

$$ik\widetilde{E_1} = \frac{q_s}{\varepsilon_0}(\widetilde{n_{r,1}} - \widetilde{n_{l,1}}) \tag{19}$$

Eliminating all perturbation terms and introducing the plasma frequency, $\omega_p = \sqrt{\frac{q^2 n_0}{\varepsilon_0 m_e}}$ results in the dispersion relation,

$$1 = \frac{\omega_p^2}{(\omega - v_0 k)^2} + \frac{\omega_p^2}{(\omega + v_0 k)^2} \tag{20}$$

Rearranging the terms in the dispersion relation and introducing a new variable, x = ω^2 results in the following form.

$$x^2 - 2x(\omega_p^2 + v_0^2 k^2) + v_0^4 k^4 - 2\omega_p^2 v_0^2 k^2 = 0 \tag{21}$$

The imaginary solutions of this equation indicates the instabilities. We need to take the solution of x with a minus sign. So in our case x is equal to

$$x = v_0^2 k^2 + w_p^2 - w_p^2\sqrt{1 + \frac{4v_0^2 k2}{w_p^2}} \tag{22}$$

Imaginary solutions for ω are obtained if x is negative, so we need to restrict wave number k and find its range in which x will be negative.

$$v_0^2 k^2 + w_p^2 - w_p^2\sqrt{1 + \frac{4v_0^2 k^2}{w_p^2}} < 0 \tag{23}$$

From this equation we get

$$v_0^2 k^2 (v_0^2 k^2 - 2\omega_p^2) < 0 \tag{24}$$

$v_0^2 k^2$ is always positive, so $v_0^2 k^2 - 2\omega_p^2$ must be negative, from here we get the condition for k,

$$k < \sqrt{2}\frac{\omega_p}{v_0} \tag{25}$$

$\omega(k)$ is equal to

$$\omega(k) = \omega_p\sqrt{1 + \frac{v_0^2 k^2}{w_p^2} - \sqrt{1 + \frac{4v_0^2 k^2}{w_p^2}}} \tag{26}$$

If we want to calculate maximum growth rate of our instability we need to maximize $\omega(k)$

$$\frac{d\omega(k)}{dk} = 0 \tag{27}$$

$$\frac{d\omega(k)}{dk} = \frac{\omega_p}{2} \frac{2\frac{v_0^2k^2}{w_p^2} - \frac{4\frac{v_0^2k^2}{w_p^2}}{\sqrt{1+\frac{4v_0^2k^2}{w_p^2}}}}{\sqrt{1+\frac{v_0^2k^2}{w_p^2}} - \sqrt{1+\frac{4v_0^2k^2}{w_p^2}}} = 0 \tag{28}$$

The numerator must be zero, so

$$2\frac{v_0^2k^2}{w_p^2} = \frac{4\frac{v_0^2k^2}{w_p^2}}{\sqrt{1+\frac{4v_0^2k^2}{w_p^2}}} \tag{29}$$

From here we get that $k = \sqrt{3}\frac{\omega_p}{2v_0}$

$$\omega(k)|_{k=\sqrt{3}\frac{\omega_p}{2v_0}} = \frac{1}{2}\omega_p \tag{30}$$

3 General approach

After considering the Newtonian one dimensional two stream instability we need a generalized approach for the development of all possible instabilities that can occur in a system of counter streaming cold beam plasma beams. In this approach we are not considering the relativistic case. Consider an x-z coordinate system with wave vector $\mathbf{k} = (k_x, 0, k_z)$. For simplicity of the calculations, assume periodicity in the y direction. Consider the case of two counter streaming beams of electrons of equal density, with a background of immobile protons. Assume that the beams are travelling in the z-direction. Now consider the Euler's equations:

$$\frac{\partial n_s}{\partial t} + \nabla \cdot (n_s \mathbf{v}_s) = 0 \tag{31}$$

$$m_s \frac{\partial \mathbf{v}_s}{\partial t} + m_s (v_s \cdot \nabla)\mathbf{v}_s = q_s(\mathbf{E} + \mathbf{v}_s \times \mathbf{B}) \tag{32}$$

Along with Maxwell's equations:

$$\mu_0 \varepsilon_0 \frac{\partial \mathbf{E}}{\partial t} = \nabla \times \mathbf{B} - \mu_0 \sum_s q_s n_s \mathbf{v}_s \tag{33}$$

$$\frac{\partial \mathbf{B}}{\partial t} = -\nabla \times \mathbf{E} \tag{34}$$

Now we introduce the perturbations to the system with arbitrary fluctuations.Assume the initial state which is in equilibrium, where $n_r = n_l = n_0, \mathbf{v}_r = -\mathbf{v}_l = \mathbf{v}_0$ with $\mathbf{E}$ and $\mathbf{B} = 0$. Also assume that the beams are travelling in the z-direction,hence, $\mathbf{v}_0 = (0, 0, v_0)$. The equilibrium of each species is perturbed.Let the multidimensional perturbations be,

$$n_s \to n_{s,0} + n_{s,1}(\mathbf{x}, t) \tag{35}$$

$$\mathbf{v}_s \to \mathbf{v}_{s,0} + \mathbf{v}_{s,1}(\mathbf{x}, t) \tag{36}$$

$$\mathbf{E} \to E_0 + E_1(\mathbf{x}, t) \tag{37}$$

$$\mathbf{B} \to B_0 + B_1(\mathbf{x}, t) \tag{38}$$

Introducing these quantities and ignoring all the higher order terms in the Euler and Maxwell's equations results in the

linearized equations. The linearized Euler's equations for the two counter streaming electron beams,

$$\frac{\partial n_{r,1}}{\partial t} + n_0 \nabla \cdot v_{r,1} + v_0 \nabla \cdot n_{r,1} = 0 \tag{39}$$

$$\frac{\partial n_{l,1}}{\partial t} + n_0 \nabla \cdot v_{l,1} - v_0 \nabla \cdot n_{l,1} = 0 \tag{40}$$

$$m_s \frac{\partial \mathbf{v}_{r,1}}{\partial t} + m_s (v_0 \nabla \cdot v_{r,1}) = q_s (\mathbf{E}_1 + \mathbf{v}_{r,1} \times \mathbf{B}_1) \tag{41}$$

$$m_s \frac{\partial \mathbf{v}_{l,1}}{\partial t} - m_s (v_0 \nabla \cdot v_{l,1}) = q_s (\mathbf{E}_1 - \mathbf{v}_{l,1} \times \mathbf{B}_1) \tag{42}$$

$$\mu_0 \varepsilon_0 \frac{\partial \mathbf{E}_1}{\partial t} = \nabla \times \mathbf{B}_1 - \mu_0 q_s \left[n_0 (\mathbf{v}_{r,1} + \mathbf{v}_{l,1}) + \mathbf{v}_0 (n_{r,1} - n_{l,1}) \right] \tag{43}$$

$$\frac{\partial \mathbf{B}_1}{\partial t} = -\nabla \times \mathbf{E}_1 \tag{44}$$

Considering the multi-dimensionality and assuming a wave like behaviour for all the perturbed quantities,

$$n_1(\mathbf{x},t) \propto \widetilde{n_1} \exp^{i(\mathbf{kx}-\omega t)} \tag{45}$$

$$v_1(\mathbf{x},t) \propto \tilde{v_1} \exp^{i(\mathbf{kx}-\omega t)} \tag{46}$$

$$E_1(\mathbf{x},t) \propto \tilde{E_1} \exp^{i(\mathbf{kx}-\omega t)} \tag{47}$$

$$B_1(\mathbf{x},t) \propto \tilde{B_1} \exp^{i(\mathbf{kx}-\omega t)} \tag{48}$$

Here $\mathbf{x}$ represents the three dimensions we consider. Substituting the above, perturbed quantities into the linearized equations and considering the fact that wave like behaviour implies, $\frac{\partial}{\partial t} \to -i\omega$ and $\nabla \to i\mathbf{k}$, we get expressions for perturbed quantities: $\widetilde{n_{r,1}}$, $\widetilde{n_{l,1}}$, $\widetilde{v_{r,1}}$ and $\widetilde{v_{l,1}}$.

$$\widetilde{n_{r,1}} = \frac{n_0 \mathbf{k} \widetilde{v_{r,1}}}{\omega - v_0 \mathbf{k}} \tag{49}$$

Similarly for left,

$$\widetilde{n_{l,1}} = \frac{n_0 \mathbf{k} \widetilde{v_{l,1}}}{\omega + v_0 \mathbf{k}} \tag{50}$$

Simplification of the other linearized equations by considering the wave like behaviour results in the following set of equations,

$$\widetilde{\mathbf{v}_{r,1}} = \frac{iq}{m\omega(\omega - \mathbf{v}_0 \mathbf{k})} \left[\mathbf{E}_1 + \mathbf{v}_0 \times (\mathbf{k} \times \mathbf{E}_1) \right] \tag{51}$$

$$\widetilde{\mathbf{v}_{l,1}} = \frac{iq}{m\omega(\omega + \mathbf{v}_0 \mathbf{k})} \left[\mathbf{E}_1 - \mathbf{v}_0 \times (\mathbf{k} \times \mathbf{E}_1) \right] \tag{52}$$

The final aim is to obtain a relation only involving $\mathbf{E}_1$. In order to do so, we use the above expressions for perturbed quantities and finally arrive at one equation containing $\widetilde{\mathbf{E}_1}$. In this final equation we use the following expressions: $c = \sqrt{\mu_0 \varepsilon_0}$ and the plasma frequency, $\omega_p = \sqrt{\frac{q^2 n_0}{\varepsilon_0 m_e}}$. The final equation in E_1 is,

$$\widetilde{\mathbf{E}_1} = -\frac{1}{c^2 \omega^2} \left[\mathbf{k} \times (\mathbf{k} \times \mathbf{E}_1) + \mathbf{v}_0 \times (\mathbf{k} \times \widetilde{\mathbf{E}_1}) \right] \frac{4 \vec{v_0} \vec{k} \omega_p^2}{(\omega^2 - v_0^2 k^2)^2} + \frac{2(\omega^2 + v_0^2 k^2) \omega_p^2}{(\omega^2 - v_0^2 k^2)^2} \widetilde{\mathbf{E}_1} \tag{53}$$

4 Two-stream Instability

After obtaining the final expression for E_1 we need to introduce some assumptions in order to get two-stream instability. We assume, that $\mathbf{k} \parallel v_0$, this implies that $k_x = 0$. This means that beams are aligned with wave vector direction. If we use

this condition we can write E_1 in components.

$$\text{x: } \widetilde{E_{1,x}}\left(1-\frac{k_z^2}{c^2\omega^2}-\frac{2(\omega^2+v_0^2k^2)\omega_p^2}{(\omega^2-v_0^2k^2)^2}\right)=0 \tag{54}$$

$$\text{y: } \widetilde{E_{1,y}}\left(1-\frac{k_z^2}{c^2\omega^2}-\frac{2(\omega^2+v_0^2k^2)\omega_p^2}{(\omega^2-v_0^2k^2)^2}\right)=0 \tag{55}$$

$$\text{z: } \widetilde{E_{1,z}}\left(1-\frac{2(\omega^2+v_0^2k^2)\omega_p^2}{(\omega^2-v_0^2k^2)^2}\right)=0 \tag{56}$$

We can write this in a tensor form:

$$\begin{bmatrix} 1-\frac{k_z^2}{c^2\omega^2}-\frac{2(\omega^2+v_0^2k^2)\omega_p^2}{(\omega^2-v_0^2k^2)^2} & 0 & 0 \\ 0 & 1-\frac{k_z^2}{c^2\omega^2}-\frac{2(\omega^2+v_0^2k^2)\omega_p^2}{(\omega^2-v_0^2k^2)^2} & 0 \\ 0 & 0 & 1-\frac{2(\omega^2+v_0^2k^2)\omega_p^2}{(\omega^2-v_0^2k^2)^2} \end{bmatrix}\begin{bmatrix} E_{x,1} \\ E_{y,1} \\ E_{z,1} \end{bmatrix}=0$$

In order to get nontrivial solution det(**T**) = 0.

$$det(\mathbf{T}) = T_{xx} * T_{yy} * T_{zz} = 0 \tag{57}$$

From given tensor we can see that $T_{xx} = T_{yy}$ and they differ with only one term from T_{zz}. So either $T_{xx} = T_{yy} = 0$ or $T_{zz} = 0$, because they can't be 0 at the same time. If we analyze T_{xx} we will see immediately that we don't get any negative solutions, therefore we don't get any instabilities. Thus, we need to investigate $T_{zz} = 0$. This implies:

$$1-\frac{2(\omega^2+v_0^2k^2)\omega_p^2}{(\omega^2-v_0^2k^2)^2}=0 \tag{58}$$

If we rearrange terms we get

$$\omega^4-2\omega^2(v_0^2k^2+\omega_p^2)+v_0^4k^4-2\omega_p^2v_0^2k^2=0 \tag{59}$$

Which is exactly the same as a simple derivation of two-stream instability. Therefore we can assume that $k \parallel v_0$ assumption leads to simple two-stream instability.

5 Filamentation instability

Since we are considering general case, we are also developing electromagnetic fluctuations, therefore we don't restrict our field to be electrostatic. In this approach, we will be able to consider all types of instabilities of 2 counter-streaming plasma beams. In our main consideration we assumed that **k** = $(k_x, 0, k_z)$, this assumption implies that our quantities won't depend on y. We follow the exact same procedures as shown in paragraph 2 (General approach) and therefore, arrive at the same final equation 53. we need to make some assumptions in order to get filamentation instability. We are going to analyze the case where $\mathbf{k} \perp v_0$, which implies that $k_x = 0$, because at the beginning we assumed that $v_0 = (0, 0, v_0)$. After setting this condition, it means that we get beams perpendicular to the wave vector. At some point, this assumption eases the work, because most of the **k** * v_0 terms cancel out. When we use this condition in the general E_1 equation we write it in the following form $\mathbf{T}*\mathbf{E}^1 = 0$:

$$\begin{bmatrix} 1-\frac{2\omega_p^2}{\omega^2} & 0 & 0 \\ 0 & 1-\frac{k_x^2}{c^2\omega^2}-\frac{2\omega_p^2}{\omega^2} & 0 \\ 0 & 0 & 1-\frac{k_x^2}{c^2\omega^2}-\frac{2\omega_p^2}{\omega^2}-\frac{2\omega_p^2}{\omega^4}v_0^2k_x^2 \end{bmatrix}\begin{bmatrix} E_x^1 \\ E_y^1 \\ E_z^1 \end{bmatrix}=0$$

Where our final tensor is :

$$\mathbf{T}=\begin{bmatrix} 1-\frac{2\omega_p^2}{\omega^2} & 0 & 0 \\ 0 & 1-\frac{k_x^2}{c^2\omega^2}-\frac{2\omega_p^2}{\omega^2} & 0 \\ 0 & 0 & 1-\frac{k_x^2}{c^2\omega^2}-\frac{2\omega_p^2}{\omega^2}-\frac{2\omega_p^2}{\omega^4}v_0^2k_x^2 \end{bmatrix} \tag{60}$$

T is the tensor. If we want to get nontrivial solution, determinant of **T** tensor must be 0.

$$det(\mathbf{T}) = T_{xx} * T_{yy} * T_{zz} = 0 \tag{61}$$

Since we are looking for instabilities we need to find imaginary solutions to the equation. Condition $T_{xx} = 0$ implies that

$$\omega^2 = 2 * \omega_p^2 \tag{62}$$

which doesn't give imaginary solutions. The same goes for $T_{yy} = 0$,

$$1 - \frac{k_x^2}{c^2\omega^2} - \frac{2\omega_p^2}{\omega^2} = 0 \tag{63}$$

arranges to

$$\omega^2 = 2\omega_p^2 + \frac{k_x^2}{c^2} \tag{64}$$

Such ω is always positive, so we don't get any imaginary solutions.
The most important and interesting is $T_{zz} = 0$.

$$1 - \frac{k_x^2}{c^2\omega^2} - \frac{2\omega_p^2}{\omega^2} - \frac{2\omega_p^2}{\omega^4} v_0^2 k_x^2 = 0 \tag{65}$$

After solving the 4^{th} order polymonial, we get that

$$\omega^2 = \frac{1}{2}\left(2\omega_p^2 + \frac{k_x^2}{c^2} - 2\omega_p^2\sqrt{1 + \frac{k_x^2}{\omega_p^2 c^2} + 2\frac{v_0^2 k_x^2}{\omega_p^2} + \frac{k_x^4}{4c^4\omega_p^4}}\right) \tag{66}$$

Since we are looking for imaginary solutions ω must fulfill the condition

$$\omega^2 < 0 \tag{67}$$

After rearranging the terms we get that we have instabilities for all k-s and therefore solutions don't need to be restricted, the way we had to do for parallel approximation. If we plot the given ω^2 versus k, we can see the behavior of our ω in Figure 1.

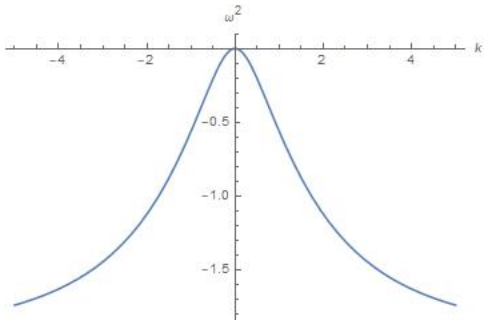

Figure 1: ω^2 dependence on k.

In order to get the maximum growth rate of the system, we need to take the limit of our ω^2 : $\lim_{x\to\infty} \omega^2 = -2v_0$. Therefore we obtain the maximum growth rate for a specific area, which has the most interesting profile.

6 Code Features

6.1 Introduction

Theoretically, the code that needed to be developed solves the Vlasov-Maxwell system of equations which, of course, consists out of the Vlasov equation. This equation describes the time evolution of the distribution function of plasma

$$\frac{\partial f_s}{\partial t} + \vec{v} \cdot \frac{\partial f_s}{\partial x} + \frac{q_s}{m_s}\left(\vec{E} + \vec{v} \times \vec{B}\right) \cdot \frac{\partial f_s}{\partial \vec{v}} = 0 \tag{68}$$

And the Maxwell equations, which govern the Electric and Magnetic field, are given by:

$$\begin{aligned} \varepsilon_0 \nabla \cdot \vec{E} &= \sum_s \rho_s \\ \nabla \cdot \vec{B} &= 0 \\ \frac{\partial \vec{B}}{\partial t} &= -\nabla \times \vec{E} \\ \mu_0 \varepsilon_0 \frac{\partial \vec{E}}{\partial t} &= \nabla \times \vec{B} - \mu_0 \sum_s J_s \end{aligned} \tag{69}$$

In which the sources are computed from the distribution function of each species:

$$\begin{aligned} \rho_s(\vec{x},t) &= q_s \int f_s(\vec{x},\vec{v},t) d\vec{v} \\ J_s(\vec{x},t) &= q_s \int f_s(\vec{x},\vec{v},t) \vec{v} d\vec{v} \end{aligned} \tag{70}$$

Naturally, developing a program that can solve these equations in 3D is extremely difficult and likely cannot be done in several weeks. Consequently, we did the next best thing. We started by programming the simplest Particle-in-Cell algorithm, or PiC for short, and, as long as time permitted, made it more and more complex. This lead us, as you will see later on, from a 1D Electrostatic to a 1D3V Electromagnetic PiC algorithm.

6.2 Electrostatic PIC

Starting off, the first PiC that was programmed is, of course, a 1D Electrostatic PiC. In this program the system is assumed to be one-dimensional and variation of the parameters only occurs in that same direction. Furthermore, it is assumed that no magnetic fields are present. With these assumptions, one then finds that the Maxwell equations reduce to:

$$\frac{\partial E}{\partial t} = -J \tag{71}$$

Where J is the current produced by the particle motions. Note, in this formula and every formula further on the units are assumed to be in SI and a normalization is used, such that, $c = \mu_0 = \varepsilon_0 = 1$. Lastly, the particles are considered to move with non-relativistic speeds. Naturally, their movement is then given by the Newton equations of motion.

$$\begin{aligned} \frac{dx_p}{dt} &= v_p \\ \frac{dv_p}{dt} &= \frac{q_p}{m_p} E \end{aligned} \tag{72}$$

These above equations are the ones our Particle-in-Cell program needs to solve numerically, which is done by employing a finite-difference discretization in time and space. The discretization in space is done with the help of a computational grid, which consists out of N_g cells and $N_g + 1$ nodes. On these nodes the discrete electric field E_g is defined. The discrete system of equations is then given by:

$$\begin{aligned} \frac{E_g^{n+1} - E_g^n}{\Delta t} &= -J_g^n \\ \frac{x_p^{n+1} - x_p^n}{\Delta t} &= v_p \\ \frac{v_p^{n+1} - v_p^n}{\Delta t} &= \frac{q_p}{m_p} E_p^n \end{aligned} \tag{73}$$

Where the subscript g denotes the quantities which are defined at the node and the subscript p denotes those that are defined at the particle position. Another important thing to note here is that the particles in the program are not physical particles, but instead represent a collection of physical particles which behave in the same way. The reason for this is simple, a plasma normally contains a huge amount of particles and solving the above discrete equations for each one of these particles every time step would be incredibly time consuming. Luckily, by using a limited amount of "Macro-particles" one can already obtain results which correspond to reality.

Lastly, equations for the current J_g and the Electric field energy at the particle position E_p are needed. These are given by:

$$\begin{aligned} J_g &= \frac{1}{\Delta x}\sum_p q_p v_p W_{pg}(x_p - x_g) \\ E_p &= \sum_g E_g W_{pg}(x_p - x_g) \end{aligned} \tag{74}$$

Where q_p is the particle charge, v_p is the particle velocity, $Deltax$ is the cell length, E_g is the electric field in the grid nodes and W_{pg} is an appropriate interpolating algorithm. The program, thus, uses the information from the particles to calculate the current, which drives the evolution of the electrical field on the grid E_g. For the interpolation function W_{pg}, first order b-splines are used, which is given by:

$$W_{pg}(x_p - x_g) = \begin{cases} 1 - \frac{|x_p - x_g|}{\Delta x} if |x_p - x_g| < \Delta x \\ 0 \text{ otherwise} \end{cases} \tag{75}$$

This expression means that when a particle at position x_p is considered, it will receive information from all the grid nodes that are less far than a distance Δx. Conversely, the same is true when a node at positions x_g is considered to gather information from the surrounding particles. Using the previous expression, the equation for the electric field in 74 can be rewritten to:

$$E_p = E_i\left(1 - \frac{|x_p - x_i|}{\Delta x}\right) + E_{i+1}\left(1 - \frac{|x_p - x_{i+1}|}{\Delta x}\right) \tag{76}$$

$$= E_i\left(1 - \frac{x_p - x_i}{\Delta x}\right) + E_{i+1}\frac{x_p - x_i}{\Delta x} \tag{77}$$

where i is the index of the node to the left of the particle and i+1 is the one of the right node. For the current this will work a bit differently. The reason for this, is that each node will receive information from the particles surrounding it. The problem, however, is that we do not know ahead of time how many (and which ones) will contribute to a specific node. It is, therefore, a lot easier to, instead of first looping over all the nodes combine with a nested loop over all the particles, just loop over all the particles once and add their contributions to their surrounding nodes. This results in the following equations:

$$J_i = J_i + \frac{q_p v_p}{\Delta x}\left(1 - \frac{x_p - x_i}{\Delta_x}\right) \tag{78}$$

$$J_{i+1} = J_{i+1} + \frac{q_p v_p}{\Delta x}\left(\frac{x_p - x_i}{\Delta_x}\right) \tag{79}$$

Do, however, note that before the loop one must initialize the current as zero everywhere on the grid.

In terms of equations the last thing that needs to be discussed is, of course, the boundary conditions. In this program the boundaries are considered to be continuous. This means that when the particles leave the domain 0 < x < L, they are placed back into it but at the other side. Or in terms of equations:

$$\text{if } x_p < 0\text{: } x_p = x_p + L \tag{80}$$

$$\text{if } x_p > \text{L: } x_p = x_p - L \tag{81}$$

Furthermore, the quantities defined on the grid, i.e. the electric field E_g and the current J_g, also need to be considered. With continuous boundaries the outer nodes of the domain are actually one and the same. This isn't necessarily a problem for the electric field since it can just be updated point by point via the current J_g. For the current itself, however, there will be an effect. This is caused by the fact that the formulas of 79 implies that the left most node J_0 only receives information from the particles on the right of it, but it should of course also receive information of the particles on the left of the right most

node J_{N_g+1}, due to them being considered the same node, and viceversa. Overall, this means that once the current in all grid nodes is computed, with the help of equations 79, one needs to apply the following formulas:

$$J_0 = J_0 + J_{N_g+1} \tag{82}$$

$$J_{N_g+1} = J_0 \tag{83}$$

6.2.1 Four-step PiC cycle

Lastly, lets talk about the inner workings of the program. It, naturally, starts off by initializing all the necessary quantities, such as the number of particles per cell $nppc$, the time step Δt, etc. More importantly, during this step the particle positions x_p and their velocities are initialized. For the particle positions x_p, the particles are distributed homogeneously over the domain. The initialization of the velocity, on the other hand, depends on the user. For the study conducted in this paper, we mostly looked at the Two stream instability. The program initializes this type of velocity by first distributing the velocities according to a Maxwellian. And then, subsequently adding the beam velocity v_0 to half of the particles and subtracting it from the other half.

Once the initialization is over, the time integration cycle starts. In this there are four important steps, given by:

1. Determination of the Electric field energy at the particle position E_p^n
2. Advancement of the particle positions x_p^{n+1} and velocities v_p^{n+1}
3. Determination of the new current J_g^{n+1}
4. Evolution of the Electric field E_g^{n+1}

These four steps keep on being repeated until eventually the final time step is reached and the program terminates. While the program is ongoing several quantities will be saved such as: the phase space, the Electric and Kinetic energy and the maximum velocity.

6.3 Relativistic Electrostatic PIC

The next stage in the development of the program is to modify the Electrostatic PiC so it can handle particles whose speeds are relativistic. This is relatively simple, the only thing that needs to happen for this is to rewrite the equations in terms of the momentum $u_p = \gamma_p v_p$ instead of the velocity. Starting with the equations of motion, one then finds that:

$$\begin{aligned} \frac{dx_p}{dt} &= \frac{u_p}{\gamma_p} \\ \frac{du_p}{dt} &= \frac{q_p}{m_p} E \end{aligned} \tag{84}$$

Note that γ_p is the Lorentz factor of the particle, which can be calculated from either the velocity or the momentum with the following equation:

$$\gamma_p = \frac{1}{\sqrt{1 - v_p^2}} \tag{85}$$

$$= \sqrt{1 + u_p^2} \tag{86}$$

Besides the equations of motion, only one other equation is modified, namely the first equation of 74. The result is:

$$J_g = \frac{1}{\Delta x} \sum_p \frac{u_p}{\gamma} q_p W_{pg}(x_p - x_g) \tag{87}$$

Naturally, the initialization also changes. Now, when using momenta instead of velocities, one needs to use the following formula to create two beams.

$$u_L = v_{th}\gamma_{th} - v_0\gamma_0 \tag{88}$$

$$u_R = v_{th}\gamma_{th} + v_0\gamma_0 \tag{89}$$

Where v_{th} is the Maxwellian velocity, γ_{th} is the Lorentz factor corresponding to the Maxwellian velocity, v_0 is the beam velocity and γ_0 is the Lorentz factor corresponding to the beam velocity. Also, the subscript "L" indicate the beam travelling in the negative x-direction, while "R" indicates the one travelling in the positive x-direction.

6.4 Electromagnetic PIC

Unlike the relativistic case, changing from a 1D Electrostatic PiC to a 1D 3V Electromagnetic PiC requires quite a few modifications. One of which, is that the vectors now have 3 components instead of 1. We, however, will keep the mono-dimensionality assumption, which means that the 3 components of the vectors can only vary in the x-direction. With this the Maxwell equations reduce to

$$\frac{\partial E_x}{\partial x} = \rho \tag{90}$$

$$\frac{\partial B_x}{\partial x} = 0 \tag{91}$$

$$\frac{\partial \vec{B}}{\partial t} = \frac{\partial E_z}{\partial x}\hat{j} - \frac{\partial E_y}{\partial x}\hat{k} \tag{92}$$

$$\frac{\partial \vec{E}}{\partial t} = -J_x\hat{i} - \left(\frac{\partial B_z}{\partial x} + J_y\right)\hat{j} + \left(\frac{\partial B_y}{\partial x} - J_y\right)\hat{k} \tag{93}$$

Now, note that the derivative of B_x with respect to time and space are both zero. It thus keeps its initial value, which is uniform in space, throughout the entire simulation. Also, for simplicity the divergence equation of the Electric field energy will be ignored in the implementation. Moving on, the Newton equations are now given by

$$\begin{aligned} \frac{dx}{dt} &= v_x \\ \frac{d\vec{v}}{dt} &= \frac{q}{m}\left[\vec{E} + \vec{v} \times \vec{B}\right] \end{aligned} \tag{94}$$

Another change, and probably the most important one of them all, is the fact that we will now use a staggered grid. This means that the numerical grid now consists out of 2 elements, namely grid nodes and cell centres. The cell centres, are as the name suggests located at the centres of the cell. In the program the electric field and current components are defined on the grid nodes while the magnetic field is defined on the cell centres. This type of grid is useful when approximating the spatial derivatives. The spatial derivatives on the nodes for example are easily obtained from the quantities located on the cell centres, for example:

$$\left(\frac{\partial B_z}{\partial x}\right)_i \approx \frac{B_{z,i+1/2} - B_{z,i-1/2}}{\Delta x} \tag{95}$$

Where integer indices such as "i" indicates that the quantity is defined on the node and half integer indices such as "i+1/2" and "i-1/2" indicate quantities defined on the cell centres. Of course, the spatial derivatives of the quantities on the cell centres can also be obtained easily from those on the nodes with:

$$\left(\frac{\partial E_z}{\partial x}\right)_{i+1/2} \approx \frac{B_{z,i+1} - B_{z,i-1}}{\Delta x} \tag{96}$$

With the help of these formulas, the Maxwell and Newton equations can be discretized, though we won't show the discretized formulas here.

6.4.1 Four-Step PiC Cycle

Let's now move on to the four step PiC cycle. Naturally, this also changes quite a bit, due to there now being a magnetic field. They are now given by:

1. Determination of the Electric and Magnetic field energy at the particle position: E_p^n, B_p^n
2. Advancement of the particle positions x_p^{n+1} and velocities v_p^{n+1}
3. Determination of the new current J_g^{n+1}
4. Evolution of the Electric and Magnetic field: E_g^{n+1}, B_c^{n+1}

This might, however, not seem so difficult, but there are some tricky parts. In step one for example, when trying to determine the Magnetic field energy at the particle position, one needs to note that the interpolation formula only works

for interpolation from the nodes. The magnetic field, however is defined on the cell centres. Consequently, one must first calculate the magnetic field on the node before doing the interpolation. This can be done simply by algebraic averaging:

$$B_i = \frac{B_{i+1/2} + B_{i-1/2}}{2} \tag{97}$$

Note, that this also requires boundary conditions, which are given by

$$B_0 = \frac{B_{1/2} + B_{N_g-1/2}}{2} \tag{98}$$

$$B_{N_g} = B_0 \tag{99}$$

The other tricky part, comes about in the fourth step. In this step, one needs to take extra care not to forget that the electric field also has boundary conditions. All in all, changing from a 1D-1V Electrostatic PiC to a 1D-3V Electromagnetic PiC is not difficult, though it is best to be careful when working with a staggered grid.

7 Results

We start to present our result in the order we obtain them, from the simplest electrostatic implementation (1-D 1V [1]) of the Two Stream instability to the electromagnetic implementation (1-D 3V [2]) of the Filamentation instability. Our goal is to compare the theoretical results to simulations to check the compatibility. The method followed to develop this simulation was, firstly, to verify if the instability are produced, plotting the phase space; and then adjusting the parameters to get the best result, in other words we want the instability to develop pretty clearly in the physical framework we are working in, so that it is possible to make physical considerations. Let's introduce the physical framework of the simulation. After a small perturbation our system of particles, described by a Maxwellian distribution, evolves in a state of instability. The initial small perturbations are growing in time becoming bigger and bigger. The kinetic energy of the plasma is converted in the electric (and magnetic) one until it's reached the point in which it is no longer possible to transfer energy. We get another equilibrium state to which can associate a new Maxwellian distribution, different from the previous one because it has a larger spectrum of velocity, so it is more spread.

7.1 Electrostatic implementation: Two Stream instability

7.1.1 Newtonian case

Energy is a very important tool to understand what is going on in a plasma. We studied the growth rate of the electric energy in function of time, varying the initial drift velocity of the particles.

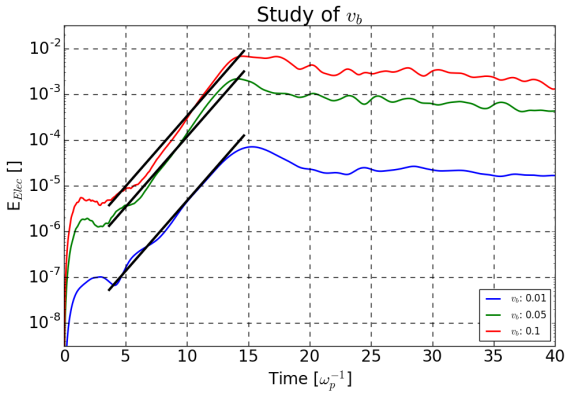

Figure 2: Fit of parametric study on v_0 (electrostatic Newtonian case) by analytical prediction (black lines)

From the calculation comes out that in the Newtonian electrostatic case the maximum growth rate ω_{max} doesn't depend on the initial drift velocity: $\omega_{max} = \frac{1}{2}\omega$; so would have the same slope in every cases. Plotting ω_{max} on our curves, we proved that's true. Thus our simulation produce the same result predicted by theory.

[1] One dimension one vector: for the velocity and the electric field

[2] One dimension three vectors: for velocity, electric and magnetic fields.

Monitoring the peaks of maximum velocity over time is another important tool in this field. The plot below shows that the maximum velocity increases in time for each value of v_0.

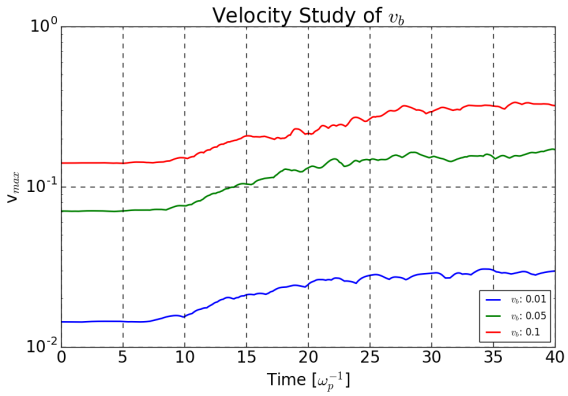

Figure 3: Display the behaviour of the maximum velocity.

That's the reason why at the end of the instability transient we have a more spread Maxwellian, so there are more particles with higher velocity than before.

7.1.2 Relativistic case

Consider now the relativistic case. Instead of the initial drift velocity we now have the parameter γ_0. In the same way electric energy is plot in function of time for different value of γ_0.

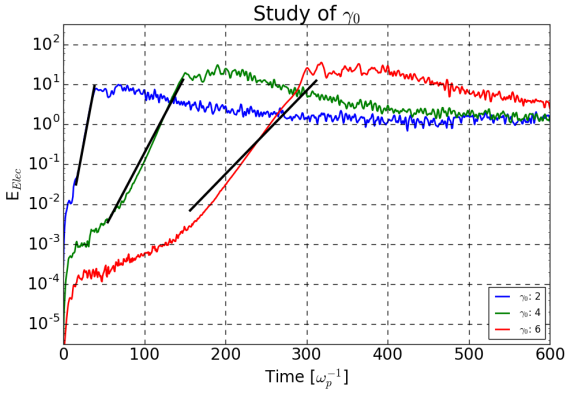

Figure 4: Fit of parametric study of γ_0 (electrostatic relativistic case) by theoretical prediction.

Here the analytical dependence of the growth rate is $\omega_{max} = \frac{w_p}{(2\gamma^{3/2})}$, depends on γ_0. From the plot it can be noticed easily that the slope changes in every case, as expected. In the study on $\gamma_0 = 6$ the slope of the expected growth rate is smaller than our curve. Despite this we reached good result from the other cases so one explanation could be given by numerical effects, but there was not enough time to prove this. Also in this case γ_{max} is growing in time like in the Newtonian case.

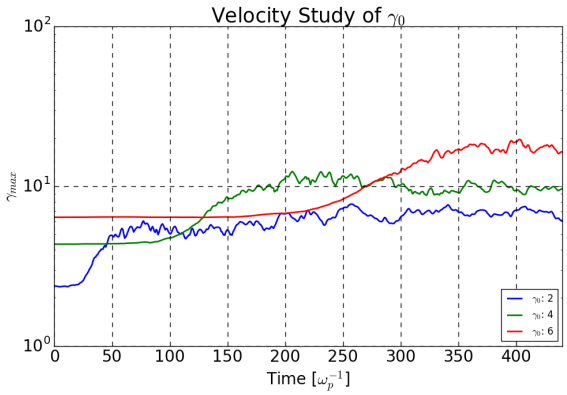

Figure 5: Behaviour of gamma maximum.

7.2 Electromagnetic implementation: Filamentation instability

Finally we present the result of the Filamentation instability. The theoretical behaviour of the growth rate, in this case, is $\omega_{max} = \sqrt{2}v_0$ so a function of the velocity.

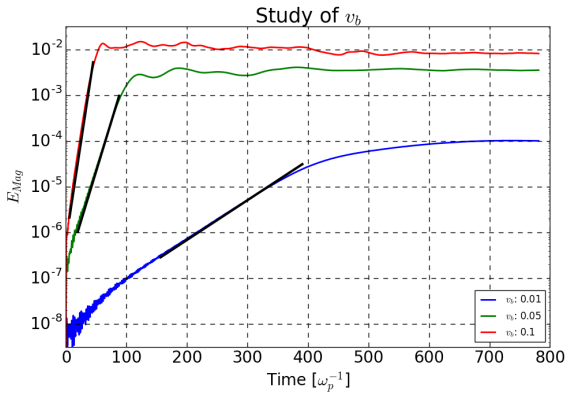

Figure 6: Fit of parametric study of v_0 for Filamentations instability.

The parametric study of v_0 shows that the slope is getting bigger, increasing the drift velocity, as we expected. Indeed perfect correspondence between simulation and reality can be observed. In the following graphics are displayed the x and y components of the maximum velocity, the z one isn't changing in time. These function are, once more, increasing in time because of instability.

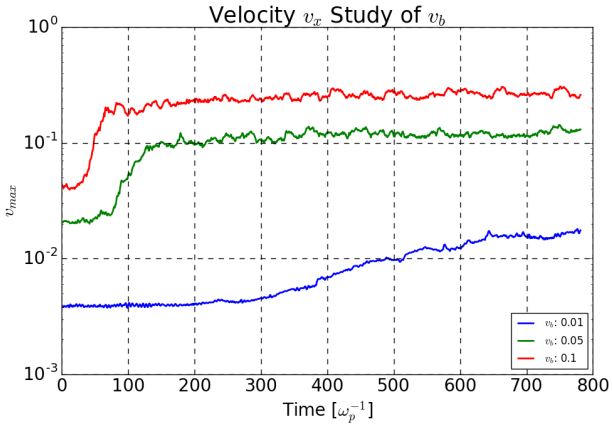

Figure 7: Monitoring the maximum velocity reached in the x direction.

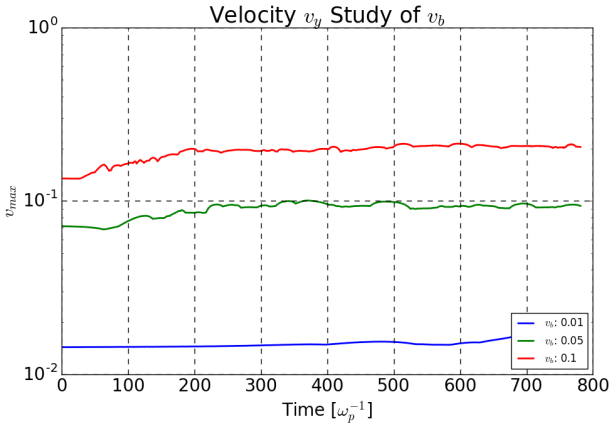

Figure 8: Monitoring the maximum velocity reached in the y direction.

8 References

1. Treumann & Baumjohann,(1997), "Advanced Space Plasma Physics," *London: Imperial College Press*, c1997
2. Medvedev, V.M & Loeb, A.(1999) "Generation of magnetic fields in the relativistic shock of gamma ray burst sources " *ApJ, 526, 697*
3. Bittencourt, J.A. (2004),"Fundamentals of Plasma Physics," Third Edition *Springer-Verlag, New York*
4. Fried, B.D. (1959), "Mechanism for Instability of Transverse Plasma Waves " *Phys. Fluids 2, 337*

8.1 APPENDIX

8.1.1 APPENDIX A: Newtonian electrostatic case

In the phase space the Two Stream instability produces, after an initial perturbation, what are called electrons hole. As you can see in the picture below, there are empty bubbles surrounded by particles: electrons in red and positrons in black.

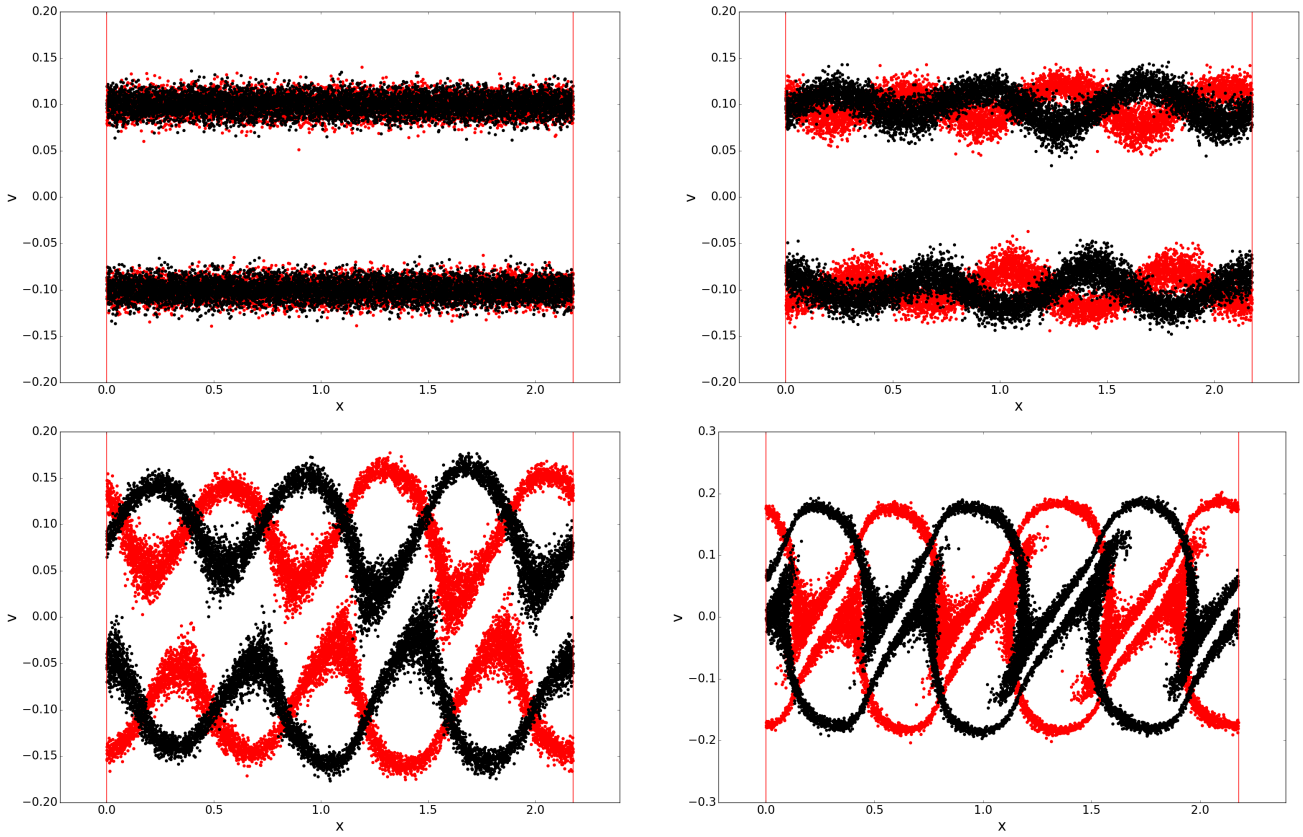

Figure 9: Electrons hole development in electrostatic Newtonian case.

The parametric analysis is fundamental in the development of a simulation. It consist in plotting our diagnostic variable (electric field, in this case) in function of time, varying a parameter with the other fixed. We did the permutations of all the simulation parameters: each case corresponds to a new configuration of the system. The goal is to get convergence in every single study, indeed curves should overlap, this means the parameters are in the best configuration possible. Below our results are shown:

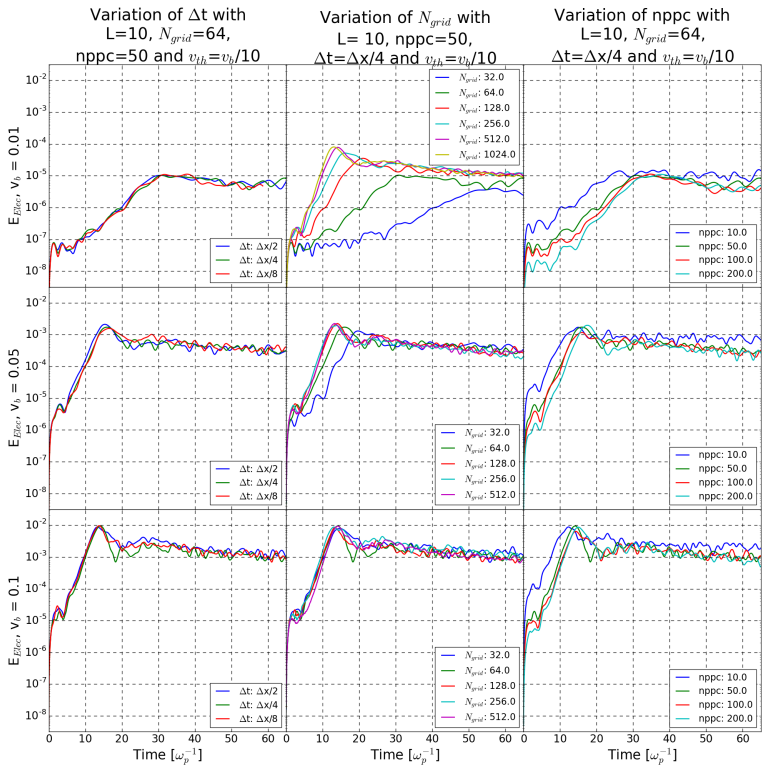

Figure 10: Parametric study for electrostatic Newtonian case.

As you can see, two parts can be distinguished in these plots: the linear development and the oscillating development. In the first one the perturbations in the plasma are growing exponentially, the kinetic energy is converted in electric energy till it reaches a new equilibrium where the plasma can be described with a new Maxwellian distribution, whose temperature is higher than the one before. We reach in almost every case a good convergence, except for the N_g study with $v_0 = 0.01$ where we can see convergence up to $N_g = 128$. So why did we choose $N_g = 64$ for the fixed parameter? The criterion to find the best simulation parameter is to take the smallest one to which we have convergence: the inferior limit; so that we could reach the best result without at the least numerical effort. Now that we have the best configuration possible, in terms of parameters:

- $N_g = 512$ [3]
- $nppc = 100$
- $\Delta t = \frac{\Delta x}{4}$

[3] We choose an higher value to get a higher accuracy and simulation is still fast.

8.1.2 APPENDIX B: Relativistic electrostatic case

Following the same procedure as before we start by checking the formation of instabilities in phase space. Then increased the value of the length domain to help instabilities grow faster. The simulation shows the following result:

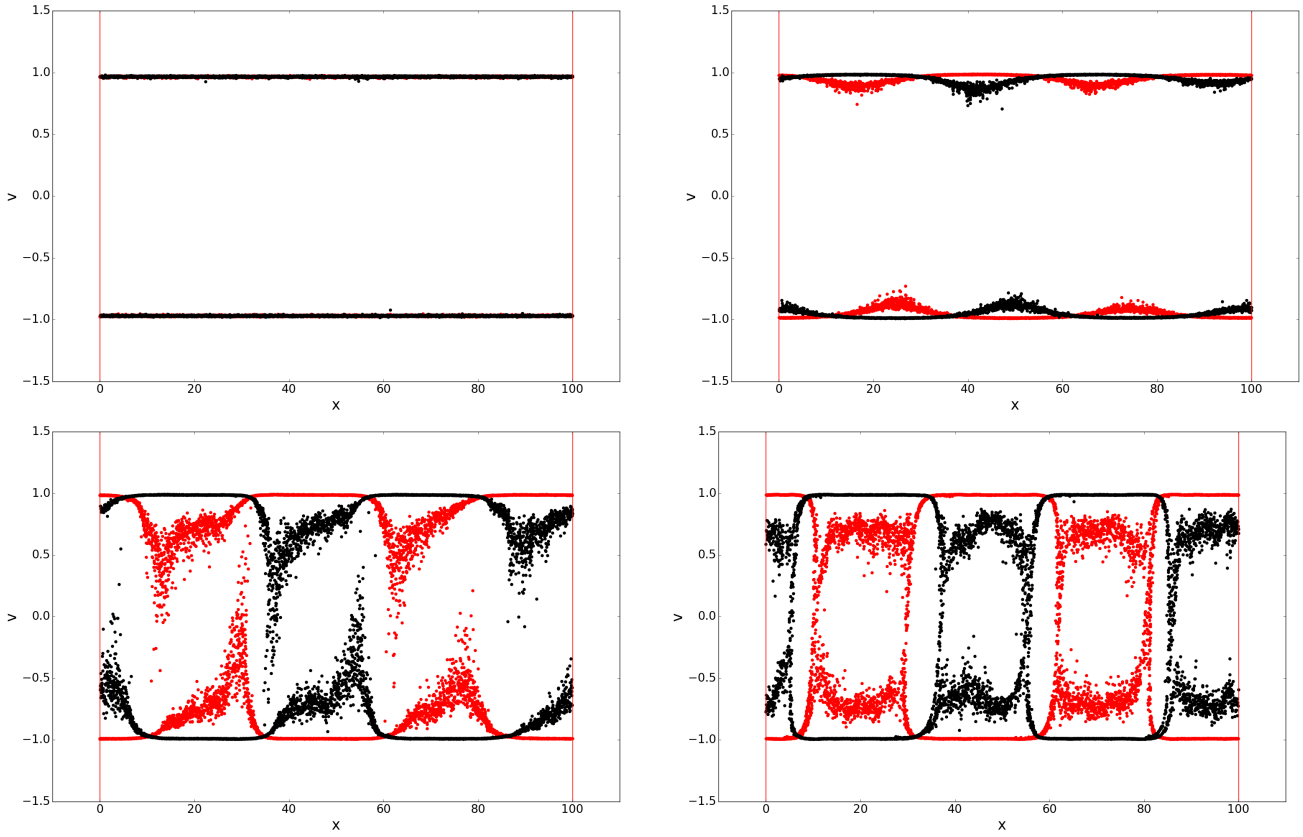

Figure 11: Electrons hole development in electrostatic relativistic case.

You notice electrons holes, in this case, use to be more square like. Since we know the best simulation parameter from the parametric analysis did before we expect to reach convergence immediately.

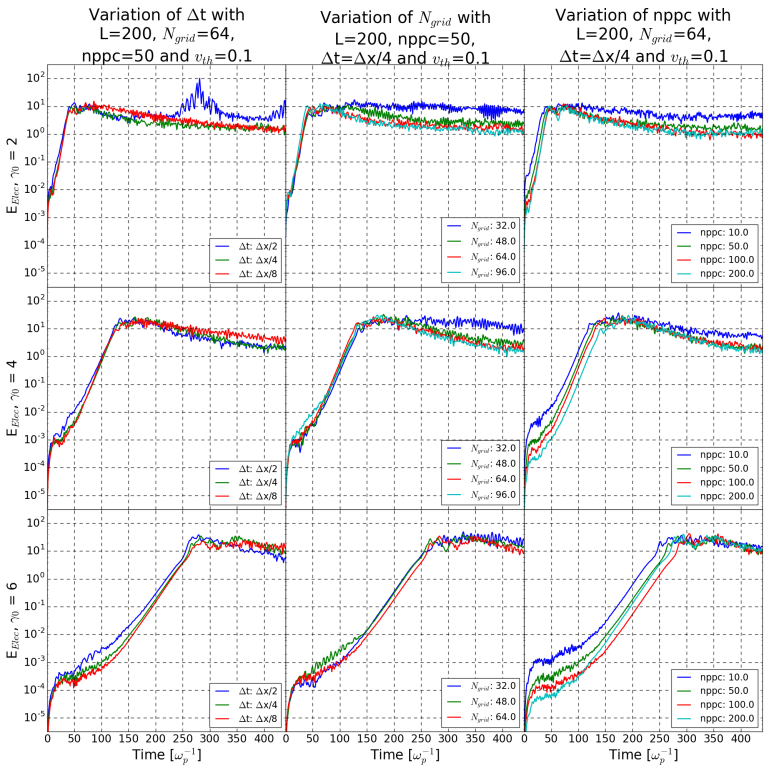

Figure 12: Parametric study of γ_0 electrostatic relativistic case

Indeed we get convergence from the first attempt. But we should be careful in the time study with $\gamma_0 = 2$, we can notice a spiky behaviour in the blue curve. We suppose the reason for this feature is only due to the fact that some particles are too fast so they skip some cell. This problem indeed is correct increasing the time step.

8.1.3 APPENDIX C: Newtonian electromagnetic case

In the electrostatic code, we only considered one component of the particle velocity, one component of the electric field vector, and one spatial dimension. Such an implementation is called "1D1V". We will now turn to a "1D3V" implementation, i.e. one spatial dimension but three components for vector quantities. We start as usual with checking the development of instabilities in phase space. From the picture below is easy to see a different topology of the instability structure, particles are thickening in some zone parallel to the y-direction, they are like fiber.

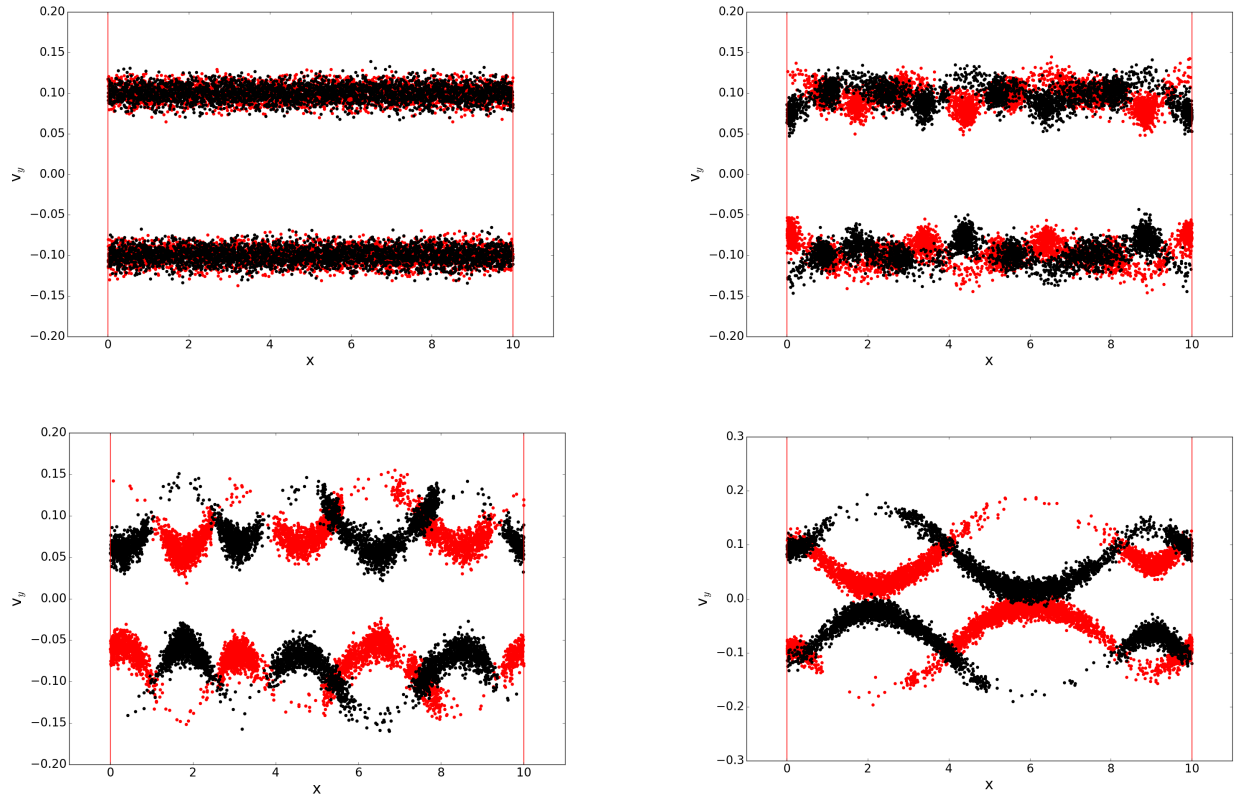

Figure 13: Filamentation instability in electromagnetic case.

Let's proceed now with the parametric study. As before we want to reach convergence in each parameter's study. We report our result in the graphic below:

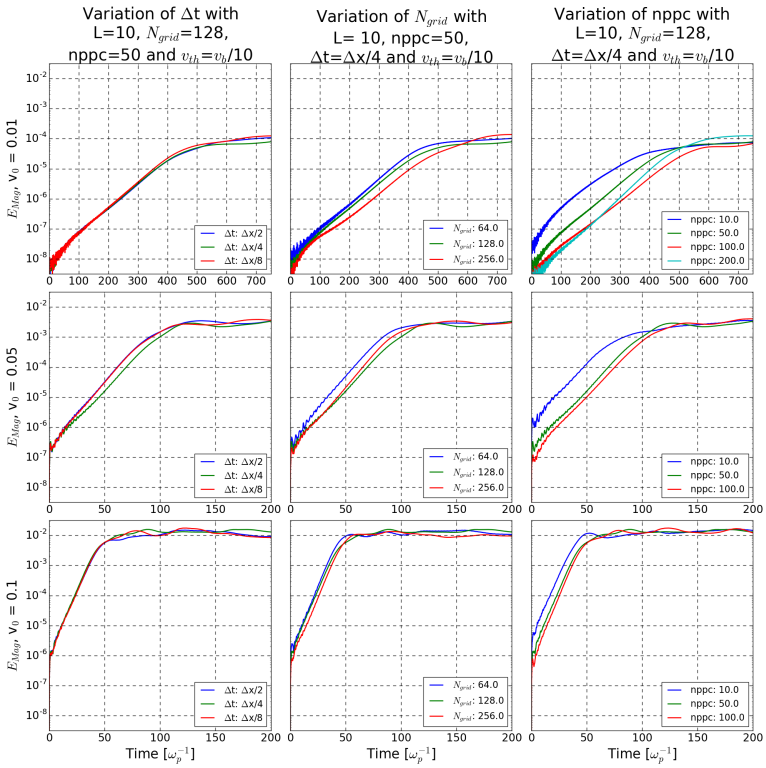

Figure 14: Electromagnetic parametric analysis.

Convergence is reached for all the parameters except for the "nppc" study where curves are a bit separated in the linear zone. For this reason we did another case with $nppc = 200$ and obtained convergence.